Partial structure factors from disordered materials diffraction data: An approach using empirical potential structure refinement

A. K. Soper
ISIS Facility, Rutherford Appleton Laboratory, Chilton, Didcot, Oxon OX11 0QX, United Kingdom
(Received 22 December 2004; revised manuscript received 13 May 2005; published 26 September 2005)

Neutron and x-ray diffraction are widely used to measure the structure of liquids and disordered solids. Using techniques such as isotope substitution or anomalous dispersion or combining neutron and x-ray data, it is sometimes possible to invert the total diffraction patterns from these materials into a set of partial structure factors, which describe the correlations between specific atom types in the material. However, even in situations where the matrix for performing this inversion appears well determined, there are significant uncertainties in the process and it is rarely possible to achieve a unique set of partial structure factors in practice. Based on the much earlier method of F. G. Edwards and J. E. Enderby [J. Phys. C **8**, 3483 (1975)] and extending the reverse Monte Carlo method of McGreevy [J. Phys.: Condens. Matter **13**, R877 (2001)] and others, a modified approach is developed here that allows possible atomic distribution functions, which are consistent with the measured data to be explored. The basis of the present approach is that any solution to the inversion process must be derivable from a distribution of nonoverlapping atoms or molecules as in the physical system under investigation. Solutions to the problem of inverting the measured differential cross sections to partial structure factors are then extracted assuming different levels of confidence in the data, confidence being represented by a feedback factor on a scale of 0–1. These different solutions serve to identify where ambiguities exist in the derived partial structure factors, particularly when a particular partial structure factor contributes only weakly to the total diffraction pattern. The method is illustrated using some old diffraction data on molten zinc chloride that have significant uncertainties associated with them, but that have been used extensively as the basis for a number of computer simulations of this material.

DOI: 10.1103/PhysRevB.72.104204 PACS number(s): 61.12.Ld, 61.20.Ja, 61.20.Qg

I. INTRODUCTION

Ever since the pioneering work of Enderby *et al.*,[1] the use of neutron scattering combined with isotope substitution has become a standard tool for elucidating structural information in multicomponent disordered materials. Fundamentally, the idea is simple: the measured structure factor $D(Q)$ is represented as a weighted sum of partial structure factors (PSF), $S_{\alpha\beta}(Q)$, with weights determined by the products of the atomic fraction c_α and scattering length b_α, of each component

$$D(Q) = \sum_{\alpha,\beta\geqslant\alpha} (2-\delta_{\alpha\beta}) c_\alpha c_\beta b_\alpha b_\beta S_{\alpha\beta}(Q), \qquad (1)$$

where Q is the wave-vector change in the diffraction experiment, the Kronecker $\delta_{\alpha\beta}$ is introduced to avoid double counting atom pairs of the same type, and the partial structure factors are related to their real-space counterparts, the site-site radial distribution functions (RDF) $g_{\alpha\beta}(r)$, by a three-dimensional Fourier transform

$$S_{\alpha\beta}(Q) = \rho \int [g_{\alpha\beta}(r) - 1] \exp i\mathbf{Q}\cdot\mathbf{r} d\mathbf{r}$$

$$= 4\pi\rho \int_0^\infty r^2 [g_{\alpha\beta}(r) - 1] \frac{\sin Qr}{Qr} dr. \qquad (2)$$

The second simplifying integral is permissible here for an isotropic fluid.[2]

For neutrons, the scattering length of a particular atom can often be altered by changing the isotopic composition of that atom. It is assumed this substitution does not change the structure appreciably, which is reasonable, in general, but may not always be rigorously valid in every case (e.g., hydrogen/deuterium substitution). By measuring the diffraction patterns for a sufficient number of isotope variants of the same sample, the set of total diffraction patterns $D(Q)$ can in principle, be inverted to produce a complete set of partial structure functions and associated site-site radial distribution functions.

In practice, of course, this full inversion is only available for a limited number of samples because suitable isotopes are often not available for some or all of the atoms. However, even when only some of the atoms have suitable isotopes, useful structural information is still derivable via the "first-order difference" method,[3] or else sometimes composite partial structure factors (CPSF), which divide the total differential cross section into weighted subsets of the individual PSFs,[4] are available. An analogous process to isotope substitution is increasingly available for x-rays. This uses the anomalous change of x-ray form factor near an absorption edge.[5,6]

In both neutron and x-ray cases, there are often significant uncertainties in measuring the data in the first place and in the subsequent data handling. These mean that the formally trivial process of inverting Eq. (1), given a suitable set of isotopic or anomalous dispersion x-ray data, is very far from trivial in practice. In particular, the primary issue to be addressed here is the extent to which any particular solution to the inversion process be justified, given the measured data. It is natural to think we approach these matters with an open

mind and, therefore, should let the experiment tell us the answer without any preconceptions. In practice, this is mostly impossible to achieve for the complex materials that form the subject of modern investigations simply because the available diffraction contrasts are not adequate to completely specify the full set of $S_{\alpha\beta}(Q)$'s.

A wide-ranging review of many of the salient issues relating to the inversion of diffraction data to real-space functions has recently been given by McGreevy.[7] A fundamental thesis of that review, and much of the work that led up to it, is that in order to have any confidence in what can and cannot be said about the structure of a disordered material on the basis of a set of diffraction data, it is important to undertake some form of structural modeling to build in known constraints on the structure, such as the number density and the fact that atoms cannot overlap. The review concentrates on the use of reverse Monte Carlo methods (RMC) to achieve this goal, but also mentions other approaches, such as the present one, empirical potential structure refinement (EPSR). The review has recently been complemented by an extensive compilation of new results using these methods.[8] A comparison and discussion of RMC and EPSR is given in Sec. V of the current paper. Indeed, it should be emphasized that EPSR evolved out attempts to use RMC to perform structure refinement on molecular systems, such as water.[9]

Whatever method is chosen to interpret diffraction data, it is well known that even when a full set of diffraction contrasts are available from experiment, the structure factors or their radial distribution functions are still subject to uncertainty because of the finite systematic errors in the diffraction experiment and the finite range of Q over which the data are available. This is particularly true when one or more of the partial structure factors makes only a weak contribution to the total diffraction pattern. In a formative paper on the partial structure factors of molten NaCl in 1975, Edwards *et al.*[10] identified the salient difficulties in extracting the partial structure factors from total diffraction data with isotope substitution (hereafter referred to as the Edwards-Enderby procedure). In essence, certain allowed limits on the possible values of the extracted partial structure factors were identified and used to eliminate unphysical solutions. In addition the low r behavior of the estimated $g_{\alpha\beta}(r)$'s was constrained to be reasonable, i.e., zero. The combination of these two sets of constraints led to a solution for both the partial structure factors and the individual radial distribution functions, which were self-consistent. The same analysis was performed on other diffraction data, including that from molten zinc chloride.[11] Overall, the proposed method of solution largely overcame weaknesses in the direct inversion process.

There is one aspect in which the Edwards-Enderby procedure can be challenged, however. As has been discussed extensively by McGreevy[7] and others for the past 15 years or so, a further constraint on possible solutions to the inversion problem is that the extracted partial structure factors and site-site radial distribution functions should be derivable from a physical distribution of atoms. (The word "physical" here is intended to indicate a three-dimensional arrangement of atoms at the correct density of the material, which involves no significant atomic overlap and reproduces the observed diffraction data as close as possible.) This is not a criticism of the Edwards-Enderby procedure but simply reflects the limitations of computing resources at the time. The procedures proposed here and elsewhere[7,8] should therefore be seen as extensions to that method, which make use of the present ready availability of computing power.

In the traditional analysis, each partial structure factor or composite partial structure factor is Fourier transformed separately (i.e., without reference to the others) to give its corresponding site-site radial distribution. However, in the real system these functions are derived from a single distribution of nonoverlapping atoms. For example, in the particular case of molten NaCl addressed by Edwards-Enderby, if a chlorine atom were to be moved, then that move would directly affect both the Na-Cl and the Cl-Cl partial structure factors because of the change in distances between these atom pairs. It might also affect the Na-Na partial structure factor indirectly because the forces acting between the Cl atom and its surrounding Na atoms might cause the surrounding Na atoms to move as well. This is the important constraint on finding solutions to the inverse problem that is not imposed in the Edwards-Enderby procedure.

Forcing the solution to be derivable from a three-dimensional distribution of atoms is, of course, no guarantee that the derived functions have any reality, but it is a *necessary* condition that any proposed solution has to satisfy. Controversy arises about how to interpret a set of diffraction data largely because different researchers do not agree on the most appropriate method to ensure the necessary conditions are met. At the time of the early isotope substitution experiments computer simulation was still in its infancy and the type of sophisticated modeling that is now possible was well beyond reach. But it is now possible to complete a simulation of simple systems, such as a molten salt, in less time than it takes to measure the diffraction data. Thus, the underlying thesis of both the RMC and EPSR methods is that any diffraction experiment that attempts to derive structure factors and radial distribution functions from a set of data should be backed up by a demonstration that the extracted functions can be generated from a physical distribution of atoms (or molecules, if present). This is especially true whenever the situation arises, as it frequently does increasingly, that there are many more site-site radial distribution functions in the system under investigation than can be measured by the isotope substitution or anomalous dispersion methods, or when one or more of those distributions is only weakly weighted in the experiment.

As a technique for making models of disordered systems, computer simulation will, of course, introduce its own approximations and uncertainties[12,13] and one is fully justified in asking whether it would not be better to investigate other integral equation methods[2] to invert the data. Indeed an extended series of articles spanning nearly four decades has attempted to do exactly this,[14–22] although even in these cases resort has usually to be made either to numerical methods or computer simulation. But computer simulation, by definition, ensures that $g(r)$ remains everywhere positive and that atomic overlap does not occur. These are important constraints that can be difficult to enforce by other methods. The systems being studied by modern diffraction experiments often involve three or more components. There is a strong case

TABLE I. Composition of $ZnCl_2$ samples used in Biggin and Enderby experiment,[11] and the neutron weightings for the different partial structure factors. The neutron weightings are based on the most recent compilation of neutron scattering lengths.[28]

Title	At.% ^{35}Cl (%)	At.% ^{37}Cl (%)	Individual PSF weighting factors (barns/sr/atom)[a] Zn-Zn	Zn-Cl	Cl-Cl
Zn35Cl2	99.3	0.7	0.0358	0.2929	0.5982
ZnMixCl2	67.7	32.3	0.0358	0.2253	0.3541
Zn37Cl2	2.7	97.3	0.0358	0.0837	0.0489

[a]1 barn$=10^{-28}$ m^2.

to say that real progress in understanding neutron and x-ray diffraction data of complex disordered materials did not occur *until* McGreevy and Pusztai[23] started building structural models of the data. In 1969, Rietveld introduced a method of refining a model crystal structure against a set of powder diffraction data.[24] Nowadays, crystallographers are routinely expected to perform some form of three-dimensional modeling prior to publication of a crystal structure. Given the availability of powerful computer simulation methods, it is not unreasonable to expect something similar to be done in the case of disordered materials. McGreevy and collaborators[7,8,25,26] with the reverse Monte Carlo (RMC) technique have achieved something closely analogous to Rietveld refinement for liquids and glasses.

The power of structure refinement is that it may lead us to conclusions different from what we get by simply inspecting the structure factors and radial distribution functions. That is because the computer simulation will, if it is set up correctly, explore a much greater range of structures than we can visualize. Even more important, the computer allows us to try out our prejudices. Toward the end of their paper on molten zinc chloride, Biggin and Enderby[11] state that "the structure of molten $ZnCl_2$ can be well explained in terms of a purely ionic model… ." Yet at no point do they actually show the consequences of applying a "purely ionic model" to their data. Therefore, given the effort and cost that goes into measuring diffraction data and the speed of modern computers, it would seem eminently sensible that some form of structure refinement, based on a three-dimensional model of the material in question, should be performed prior to drawing conclusions about the structure of the material.

In the present paper, as an example of the proposed technique using EPSR,[9,27] we have reanalyzed the original diffraction data of Biggin and Enderby[11] on molten $ZnCl_2$. The reason for this particular choice is that although the data were published some time ago, they have not thus far been fully superseded on a modern neutron diffractometer. Yet they have been the subject of extensive computer analyses, which span right up to the present (see Discussion) to try to explain how the Zn-Zn distance is almost identical to the Cl-Cl distance, in spite of the markedly different ionic charges. Nobody yet appears to have fully established the degree of uncertainty surrounding the Biggin and Enderby conclusions. It will be shown here how using EPSR, systematic errors in the diffraction data can be incorporated into the analysis in a quantitative manner and still allow the extraction of physically meaningful partial structure factors and radial distribution functions. At the same time the problem of extracting weakly weighted partial structure factors is addressed, and the method is used to establish the likely uncertainties in such quantities.

The paper also describes a slightly modified version of EPSR, hitherto unpublished, which allows the user to apply different emphases on the diffraction data using a "feedback factor" f, which lies in the range $0<f<1$; $f=0$ corresponds to having zero confidence in the accuracy of the data, and $f=1$ corresponds to having complete confidence in the data. Before describing this method, however, and showing the outcome, the consequences of assuming 100% confidence in the data are evaluated in Sec. III.

II. CONSEQUENCES OF HAVING COMPLETE CONFIDENCE IN MEASURED DATA

Table I lists the isotopic compositions of the three samples used in the Biggin and Enderby[11] experiment, as well as the corresponding neutron-weighting factor for each measured data set for the three partial structure factors (PSF), as derived from the table of neutron scattering lengths.[28] It is clear that the Zn-Zn PSF is weakly weighted compared to the Zn-Cl and Cl-Cl PSFs in all three samples. The published diffraction data were digitized using a scanner and are shown here for completeness in Fig. 1, where it can be seen they are an authentic reproduction of the original data. The error in the digitization procedure is on the order of the size of the dots in Fig. 1 of Ref. 7 and thus is smaller than the observed statistical fluctuations in the data.

If the 3×3 matrix of coefficients in Table I is represented by w_{ij}, $i,j=1,3$, then the inverse can be obtained from the condition $[w_{ji}]^{-1}\times[w_{ij}]=[\mathbf{I}]$, where $[\mathbf{I}]$ is the unit matrix. This inverse is given in Table II, which can be verified by inspection. Figure 2 shows the effect of applying the inversion matrix directly to the data of Fig. 1. It will be seen that the result, particularly for the Zn-Zn PSF, does not look at all like the PSFs shown by Biggin and Enderby[11] in their Fig. 2. This is because, as described above, Biggin and Enderby do not use a direct inversion of the data, but instead use the iterative procedure defined by Edwards *et al.*[10] In particular, we note a strong anti-correlation as a function of Q of features between the Zn-Zn and Zn-Cl PSFs, which might in-

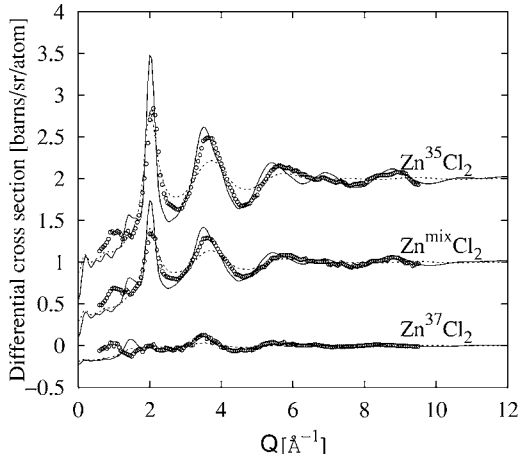

FIG. 1. Total interference differential cross sections for three samples of molten $ZnCl_2$ with different Cl isotope compositions. The compositions are given in Table I. The points show the corrected interference differential cross-sectional data for the three samples, as extracted by scanner from the original Biggin and Enderby paper.[11] The lines show the fit to these data from the "simple ion" model as described in Sec. III A. The solid line corresponds to the assumption of full ionic charges on the atoms, whereas the dashed line corresponds to assuming effective ionic charges $\frac{1}{4}$ of the full ionic values. Although the overall fit for both models is qualitatively correct, it is noticeable that the "prepeak" near 1 Å^{-1} in the data is incorrectly reproduced by either model, and many other details are missed.

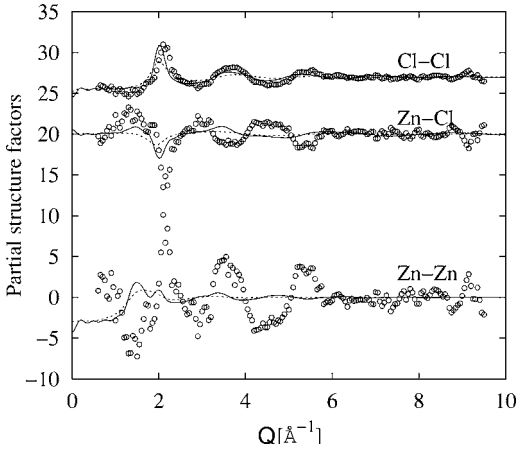

FIG. 2. Estimated partial structure factors (points) based on the diffraction data of Fig. 1 and using the direct inversion matrix, Table II. The lines show simulations of these partial structure factors based on the simple ion models as described in Sec. III and caption to Fig. 1.

dicate that the normalization of one or more of the datasets has a small error. The error only needs to be small because the size of some of the inversion coefficients (Table II) is large. It can be seen that, particularly for the Zn-Zn PSF, the inversion requires adding and subtracting the different datasets after multiplying the data by numbers as large as ~70. Because it is virtually impossible, even today, to put diffraction data on an absolute cross-section scale to better than 1–2%, it is not surprising that directly inverting the data to partial structure factors might have the effect of magnifying the systematic errors at the expense of the true signal. Indeed this conclusion is precisely in accord with the observations of Edwards-Enderby[10] for equivalent data on sodium chloride, where it was also shown that direct inversion of the data using the inversion matrix could lead to problems.

III. EMPIRICAL POTENTIAL STRUCTURE REFINEMENT (EPSR)

A. Setting up the reference potential

The first action in attempting to analyze data of this kind using EPSR is to derive a suitable reference potential, i.e., the potential energy function that will be used as the starting point for subsequent structure refinement. This can be taken from the literature, if available, or else it can be derived by inspecting the data. The latter approach is the one that was adopted here. A cubic box of 1000 Zn atoms and 2000 Cl atoms was set up, box dimension 44.7085 Å, corresponding to an assumed number density of 0.03357 atoms/Å^3. As Biggin and Enderby[11] do not state their assumed density, this value has been taken from the x-ray work of Triolo and Narten.[29] The reference potential between atom pairs was built up from a combination of Lennard-Jones and Coulomb potentials. Thus, the potential between atoms α and β would be represented by

$$U_{\alpha\beta}(r) = 4\varepsilon_{\alpha\beta}\left[\left(\frac{\sigma_{\alpha\beta}}{r}\right)^{12} - \left(\frac{\sigma_{\alpha\beta}}{r}\right)^{6}\right] + \frac{1}{4\pi\varepsilon_0}\frac{q_\alpha q_\beta}{r}, \quad (3)$$

where $\varepsilon_{\alpha\beta}=\sqrt{\varepsilon_\alpha\varepsilon_\beta}$, $\sigma_{\alpha\beta}=0.5(\sigma_\alpha+\sigma_\beta)$, and ε_0 is the permittivity of free space.

Initially all atoms were given a Lennard-Jones potential well depth, $\varepsilon_{Zn}=\varepsilon_{Cl}=0.8$ kJ/mole, with Coulomb charges of $+2e$ on the Zn atoms and $-e$ on the Cl atoms. The Lennard-Jones σ values were adjusted repeatedly until the first peak in the Zn-Cl RDF occurred at about 2.29 Å, and the first peak in the Cl-Cl RDF occurred at about 3.2 Å, as was derived in the earlier experiment.[11] This process gave σ values of $\sigma_{Zn}=1.12$ Å and $\sigma_{Cl}=4.54$ Å, respectively.

The Monte Carlo simulation itself follows the traditional pattern,[12,13] with application of periodic boundary conditions, use of the minimum image convention, and neighbor lists. To save computing time, no long-range correction to the potential energy function is made. Instead, the Lennard-Jones potential energy functions are truncated smoothly using a function of the form

TABLE II. Inversion of the matrix of coefficients of Table I.

Partial structure factor	$Zn^{35}Cl_2$	$Zn^{mix}Cl_2$	$Zn^{37}Cl_2$
Zn-Zn	37.25	−71.53	62.16
Zn-Cl	−21.87	39.37	−17.50
Cl-Cl	10.15	−14.99	4.84

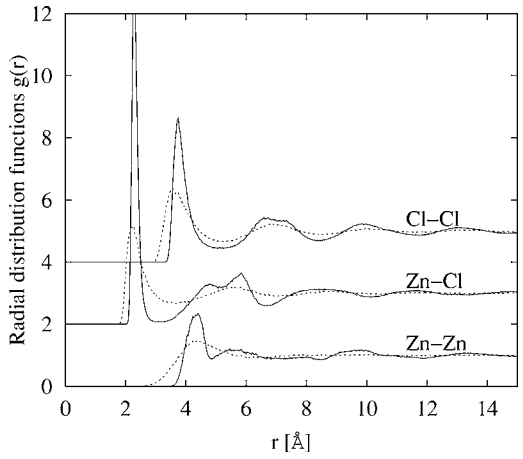

FIG. 3. Site-site radial distribution functions for the "simple ion" models of Fig. 1. The solid line corresponds to full ionic charges, and the dashed line is for when those charges are reduced to $\frac{1}{4}$ of their full values.

$$T(r) = \begin{cases} 1 & r \leqslant r_1 \\ 0.5\left[1 + \cos\,\pi\left(\dfrac{r - r_1}{r_2 - r_1}\right)\right] & r_1 < r < r_2 \\ 0 & r \geqslant r_2, \end{cases} \tag{4}$$

where $r_1 = 9$ Å and $r_2 = 12$ Å, whereas the Coulomb potentials are truncated with a function derived from the "charged clouds" interaction[30]

$$T_C(r) = \left(1 - \frac{r}{r_2}\right)^4 \left(1 + \frac{8r}{5r_2} + \frac{2r^2}{5r_2^2}\right)\Theta(r_2 - r) \tag{5}$$

with $\Theta(r_2 - r)$ the Heaviside function.

Figure 1 shows the simulated diffraction pattern versus the diffraction data for this reference potential, Fig. 2 shows the simulated partial factors compared to the direct inversion of the diffraction data, and Fig. 3 shows the simulated radial distribution functions.

This simple model could perhaps be regarded as an initial guess for the "purely ionic" model of Biggin and Enderby.[11] It clearly gets the Zn-Cl and the Cl-Cl distance reasonably accurately (Fig. 3), but that is not surprising because it was set up to do so. The Zn-Zn near-neighbor distance in the simulated distribution is, however, further out than the Cl-Cl distance, presumably because of the much greater electrostatic repulsion between the Zn atoms, together with the smaller atomic concentration, compared to the Cl atoms. This is in contrast to the results of Biggin and Enderby,[11] where it was concluded that the Zn-Zn near-neighbor distance was close to the Cl-Cl near-neighbor distance.

Of course one could reasonably argue that our chosen reference potential is too simple—ionic polarization has been ignored, for example, or the Lennard-Jones potential is possibly too repulsive at short distances—and this would make a difference to the outcome. But the point is made very clearly here that statements about the degree of ionicity in the system cannot be made simply on the basis of the position of peaks in the $g(r)$ alone. On the face of it, a simple ionic model of molten $ZnCl_2$ does not accurately reproduce the measurements. One question we will need to answer, for example, before we can analyze the data for the degree of ionicity, is how well do we actually know the Zn-Zn distance in $ZnCl_2$ liquid? Another noticeable misfit is the small peak in Q space (Fig. 1) near $Q = \sim 1$ Å^{-1}, the so-called first sharp diffraction peak (FSDP), which is not well reproduced by our initial choice of potential.

Indeed, a general comment about this initial potential for the simulation is that it produced too much structure in the simulated distributions compared to the data. To demonstrate this, a second reference potential was initiated in which the Lennard-Jones well depths were set to $\varepsilon_{Zn} = \varepsilon_{Cl} = 0.05$ kJ/mole instead of 0.8 kJ/mole as previously (i.e., a factor of 16 smaller in well depth), and the Coulomb charges were set to $+0.5e$ on the Zn atoms and $-0.25e$ on the Cl atoms, namely, a factor of 4 smaller than previously. The Lennard-Jones σ values were unchanged. The results of using this modified potential are shown as the dashed lines in Figs. 1–3 and demonstrate that, if anything, the resulting liquid now has too little structure compared to the data. Clearly therefore, there is considerable sensitivity within the data to the details of the interatomic potential. For all the subsequent structure refinements reported here, these reduced well depths and effective charges were used as the reference potentials. This was because a general rule of thumb for this kind of analysis is that the reference potential should generate, if anything, *less* structure than implied by the diffraction data rather than more, otherwise the empirical potential has to become much larger to overcome the defects in the reference potential than it would with a weaker reference potential.

B. Representing the empirical potential

It is clear from Figs. 1–3 that our initial guess for the potential, although it appears to generate a reasonable representation of the diffraction data, falls well short of producing an accurate fit. We could, in principle, attempt to refine the values of the charges and the Lennard-Jones parameters, but there is no guarantee of success if there are other factors at work besides purely Coulomb forces. We therefore need to perturb our reference potential in such a way as to make the simulated distribution functions look more similar to our measurements.

This is done via the "empirical potential"—empirical because it is derived directly from the diffraction data and has no other physical origin. A fundamental principle behind setting up the empirical potential is that it must represent only true differences between the simulation and diffraction data: it ideally should not contain any artifacts associated with the statistical noise, systematic errors, and truncation effects in the diffraction data. If it did contain these artifacts, then it is likely they will be carried over into the estimated distribution functions of the system.

In practice, this is a difficult goal to achieve and a variety of methods for generating the empirical potential (EP) have been tried. The one that appears to be most successful thus far is to expand the EP in a series of Poisson functions. This

method has not been published before and therefore is given, in detail, here. We represent the EP by a function of the form

$$U_{\mathrm{EP}}(r) = kT\sum_k C_k p_{n_k}(r,\sigma_r), \tag{6}$$

where $k=0,1,2,3,4,\ldots$,

$$p_n(r,\sigma) = \frac{1}{4\pi\sigma^3(n+2)!}\left(\frac{r}{\sigma}\right)^n \exp\left[-\frac{r}{\sigma}\right]; \tag{7}$$

the C_k are real (but can be positive or negative) and σ_r is a width function to be set by the user. The normalization in (7) arises from the requirement that $4\pi\int p_n(r,\sigma)r^2dr=1$. (Note that the width parameters (σ_r,σ_Q) described in this section have nothing to do with the Lennard-Jones parameters σ_α of the previous section: (σ_r,σ_Q) are simply width parameters, which are the same for all atom pairs.) The total atomic number density of the simulated system is ρ. It will be noted that in three dimensions, $p_n(r,\sigma)$ has a first moment of $(n+3)\sigma$ and a mean-square deviation about this value of $(n+3)\sigma^2$, which means it peaks near $r\sim n\sigma$ for large n with a width that gets gradually larger with increasing n. It is therefore a natural function to represent the interatomic potential, which tends to vary rapidly with r at shorter distances and becomes more slowly varying at longer distances.

These facts are used to generate the values of n_k in (7). Essentially, a set of radius values r_k is selected by the user to correspond with the likely range of the empirical potential, and the values of n_k corresponding to these radii are given by

$$n_k = \frac{r_k}{\sigma_r}, \quad n_k \geqslant 0. \tag{8}$$

The function $p_n(r,\sigma)$ has an exact three-dimensional Fourier transform to Q space

$$P_n(Q,\sigma) = 4\pi\int p_n(r,\sigma)\exp(i\mathbf{Q}\cdot\mathbf{r})d\mathbf{r}$$

$$= \frac{1}{(n+2)(\sqrt{1+Q^2\sigma^2})^{(n+4)}} \times\left[2\cos(n\alpha) + \frac{(1-Q^2\sigma^2)}{Q\sigma}\sin(n\alpha)\right], \tag{9}$$

where $\alpha=\arctan(Q\sigma)$. Therefore in EPSR, the coefficients C_k are estimated directly from the diffraction data by fitting a series of the form

$$U_{\mathrm{EP}}(Q) = 4\pi\int U_{\mathrm{EP}}(r)\exp(i\mathbf{Q}\cdot\mathbf{r})d\mathbf{r} = \sum_k C_k P_{n_k}(Q,\sigma_Q) \tag{10}$$

to the difference between diffraction data and simulation in Q space, and then using the C_k coefficients so generated to produce the EP in r space via Eq. (6). The values of n_k in (10) are generated by an analogous formula to (8) $n_k=r_k/\sigma_Q$. This procedure avoids the need to perform a numerical Fourier transform of the diffraction data and eliminates many of the problems associated with noise in the data and truncation ripples, which would otherwise appear.

The use of the functions, such as (7), helps to reduce the transfer of truncation effects to the empirical potential. A further degree of smoothing in the derived EP can be achieved by setting σ_r used in (6) to be *larger* than σ_Q in (10), typically a factor of 4 larger in the current version of the program. This means the values of n_k in (10) will not be the same as those used in (6), so the program does not use an exact reconstruction of the data to generate the potential. In practice, the best results are obtained with σ_Q, typically smaller than the spacing between the r values, so the primary effect of using this factor of 4 for σ_r is to broaden the reconstructed function (6) compared to what it might otherwise have been and thus make an even smoother empirical potential. In practice, the change in width in this case produces very little discernible distortion of the resulting function, but, of course, if the potential function is made too broad, then, it may prevent the best possible fit to the data being achieved. Typically, use of $\sigma_Q=0.01$ Å in (10) is found to give satisfactory results, with $\sigma_r=0.04$ Å in (6) for the reconstruction. Note also that the functional form (6) is such that gradients (forces) and higher derivatives of the potential all have analytical expressions.

C. Refining the empirical potential: Introducing the data

If there are J distinct atomic components in the system being studied, then there are $N=J(J+1)/2$ distinct site-site RDFs to be determined. We will assume that we have measured M diffraction data sets $D_i(Q)$, each with a different isotopic composition. Based on (1) the fit to the ith data set of a particular experiment can be represented by a weighted sum over all the pairs of atom types of the relevant simulated partial structure factors $S_{\alpha\beta}(Q)$

$$F_i(Q) = \sum_{j=1,N} w_{ij}S_j(Q), \tag{11}$$

where j represents one of the atomic pairs (α,β) in (1) and the weights w_{ij} are determined from the respective product of atomic fractions and neutron-scattering lengths for that particular sample as given in (1). The question is how to invert the matrix w_{ij}, in general? In the present case, $ZnCl_2$, the system of Eqs. (11) can be directly inverted to yield the partial structure factors from the data because there is a complete set of isotope data available. For most systems of experimental interest the matrix of coefficients is ill determined, making direct inversion impossible. Even in the present well-determined case, there are questions about the validity of doing this, given the weak contribution of one of the PSFs to the total diffraction pattern.

In order to cover all of the situations likely to be encountered in real experiments, we assign a feedback factor to the data f, where $0\leqslant f\leqslant 1$, and form the weights

$$w'_{ij} = fw_{ij}, \quad \text{for } 1\leqslant i\leqslant M. \tag{12}$$

In addition to these we form an additional, diagonal array of weights

TABLE III. Inversion of the weights matrix for $ZnCl_2$ for the case of $f=0.95$.

PSF	$Zn^{35}Cl_2$	$Zn^{mix}Cl_2$	$Zn^{37}Cl_2$	Zn-Zn	Zn-Cl	Cl-Cl
Zn-Zn	−0.35	−0.27	4.83	0.85	−0.24	0.07
Zn-Cl	−2.65	4.29	5.12	−0.24	0.38	−0.18
Cl-Cl	2.66	−1.53	−2.97	0.06	−0.18	0.1

$$w'_{ij} = (1-f)\delta_{(i-M),j}; \quad \text{for } M < i \leqslant (M+N). \tag{13}$$

Effectively, this additional set of weights is equivalent to saying we accept the data with feedback factor f and the simulation with feedback factor $(1-f)$. This leads to an overdetermined matrix in every case [N columns $\times (M+N)$ rows], provided $0<f<1$.

We then seek the inverse of this matrix w_{ji}^{-1} such that the $(M+N)\times(M+N)$ matrix formed from $P_{ii'}=(\Sigma_{j=1,N} w'_{ij} w_{ji'}^{-1} - \delta_{ii'})$ has a minimum norm, which gives the least-squares solution for w_{ji}^{-1} in the case of an overdetermined set of linear equations as here. This is a straightforward problem that can be solved by standard techniques, and the solution can be checked from the requirement that the matrix $P_{j'j} = \Sigma_{i=1,M+N} w_{j'i}^{-1} w'_{ij}$ must be unitary. Since the matrix w'_{ij} is always well determined from (12) and (13), there should never be a problem with singularities.

The complete algorithm for calculating the EP can now be written down. At the beginning of the mth iteration of the algorithm each distinct pair of atoms j will have a set of coefficients $C_{k,m}^{(j)}$, which are used to form the empirical potential for that atom pair. Following (6), the EP for that pair of atoms is determined from

$$U_m^{(j)}(r) = kT \sum_k C_{k,m}^{(j)} p_{n_k}(r, \sigma_r). \tag{14}$$

(At the beginning, with $m=1$, the coefficients $C_{k,m}^{(j)}$ are set to zero.) After the mth iteration, the difference between data and fit $[D_i(Q)-F_i(Q)]$, is calculated, and represented by a sum of the form (10). This gives rise to a set of difference coefficients, $C_k^{(i)}$, which change as the simulation proceeds—ideally they should go to zero when the simulation approaches the data closely. These difference coefficients are then accumulated in the potential coefficients

$$C_{k,m+1}^{(j)} = C_{k,m}^{(j)} + \sum_{i=1,M} w_{ji}^{-1} C_k^{(i)}. \tag{15}$$

The revised values $C_{k,m+1}^{(j)}$, are now used in (14) to form a new version of the EP, and the simulation is run again. This whole cycle is repeated a large number of times until one of two conditions is reached. Either the difference coefficients $C_k^{(i)}$, become insignificantly small so that the empirical potential does not change any more, or else the modulus of the empirical potential energy, defined by $\bar{U} = 4\pi\rho\Sigma_{j=1,N} |U_m^{(j)} \times (r)| g_j(r) r^2 dr$ reaches some predefined limit. The latter tends to happen when there are systematic errors in the data that cannot be fit by any potential energy function. In that case, the EP would increase in amplitude, indefinitely, if it were not capped and might introduce artifacts into the calculated distribution functions. Thus, in the EPSR approach there is still scope for subjectivity on the part of the experimenter as they may need to set a cap for the empirical potential energy modulus if systematic error is present. Indeed, the need to set a cap on the empirical potential is a likely sign of appreciable systematic error in the data.

Obtaining an inverse to our matrix of weight coefficients means we can, in the spirit of the above, also write down our best estimate of the partial structure factors based on our relative confidence in the data and the simulation

$$T_j(Q) = \sum_{i=1,M} w_{ji}^{-1} D_i(Q) + \sum_{i=M+1,M+N} w_{ji}^{-1} S_{i-M}(Q). \tag{16}$$

These estimated partial structure factors can then be compared to the simulated structure factors. As will be seen below, as f is made progressively smaller than unity, these estimated partial structure factors can appear markedly different from those obtained by assuming 100% feedback from the data. This is one way in EPSR that different distributions of atoms, each of which is compatible with the diffraction data, can be generated.

IV. DISCUSSION: RESULTS OF APPLYING EPSR TO THE BIGGIN AND ENDERBY $ZnCl_2$ DATA

The simulation (lines) shown in Figs. 1–3 is effectively the case where the feedback factor f of the previous section has been set to zero; thus, there is no confidence assigned to the data and the empirical potential is also zero. This is the case where the simulation is run with the reference potential on its own. The cases where increasing confidence is given to the data are now examined, with f taking the values 0.2, 0.4, 0.6, 0.8, 0.9, 0.95, 0.98, 0.99, and 1.0. For the Zn-Zn radial distribution function, a minimum r cutoff of 3.2 Å was imposed to prevent the Zn atoms from approaching one another too closely.

To illustrate the effect of assuming $<100\%$ confidence in the data, Table III shows the inversion matrix for the case when $f=0.95$. It is quite marked how the cofactors diminish significantly in amplitude by this simple device, for the Zn-Zn PSF, the cofactors are at least an order of magnitude smaller. This automatically means far less emphasis will be placed on the data to extract the Zn-Zn PSF compared to placing 100% confidence in the data. Note also that for the Zn-Zn PSF, there is significant dependence on the simulation (fifth column, row 2), whereas for the Cl-Cl PSF, the result is still dominated heavily by the data (row 4). This is in keeping with the relative weighting of these two terms in the differential cross sections (Table I).

For all values of f, the modulus of the empirical potential energy was capped at 100 kJ/mole, although Table IV,

TABLE IV. Quality of fit and modulus of the empirical potential energy for different values of the feedback factor f.

Feedback factor f	Quality of fit $R_f(\times 10^2)$	Modulus of empirical potential energy $\bar{U}$ (kJ/mole)
0.00	0.86	0
0.20	0.26	77
0.40	0.18	91
0.60	0.19	100
0.80	0.21	100
0.90	0.23	100
0.95	0.25	98
0.98	0.29	94
0.99	0.36	99
1.00	0.45	103

which summarizes the main outcomes, shows that for $f \leqslant 0.6$ this limiting value was never reached. In other words, the residuals $[D_i(Q)-F_i(Q)]$ had become too small to make any significant impact on the EP. The quality of fit for each value of f is reported as the unweighted sum $R_f = 1/M\Sigma_i 1/n_Q \Sigma_Q [D_i(Q)-F_i(Q)]^2$, where n_Q is the number of Q values in each dataset. Figures 4 and 5 show the fits to the differential cross section data for the cases of $f=0.4$, 0.8 and 1.0 respectively.

Table IV reveals something unexpected, namely, when the feedback factor is set below unity, the fit obtained is apparently better than when we use maximum feedback in setting up the empirical potential. The visual fits to the data (Figs. 4 and 5) bear out this conclusion. The fact that assuming $<100\%$ confidence in the data produces a better fit suggests there are residual systematic errors in the data that were not removed by the data correction procedures. These residual errors are likely to be small, otherwise it would not be possible to generate such close fits to the differential cross sections (Fig. 4). Nonetheless, when used to calculate the partial structure factors, using the direct inversion of the scattering matrix (Table II), these small errors become magnified to the point where the resulting partial structure factors are quite unphysical. Without the check of attempting to derive the measured data from a physical distribution of atoms, there would be no easy way of identifying this error.

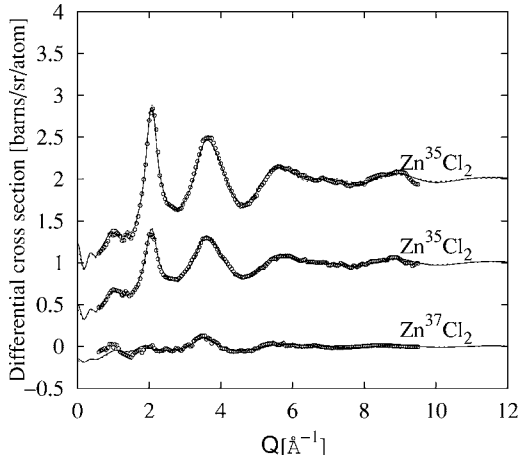

FIG. 4. Same data as Fig. 1, but now the solid lines correspond to the EPSR fit when a feedback factor $f=0.4$ is used. Note that the prepeak near 1 Å^{-1} is now correctly reproduced in the fit. The dashed line, where visible, corresponds to $f=0.8$ and is virtually indistinguishable from $f=0.4$, although according to Table IV it produces a slightly worse fit overall.

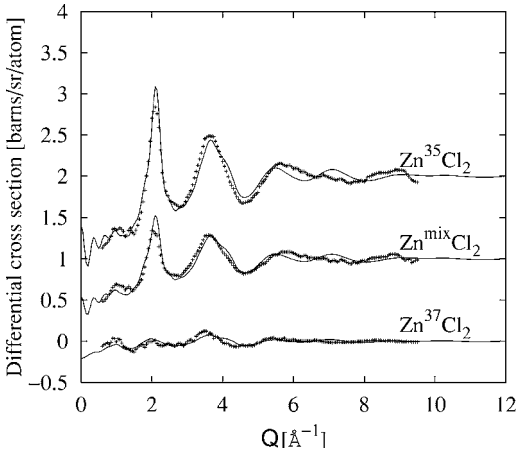

FIG. 5. Same as Fig. 1, but now the lines correspond to the EPSR fit when a feedback factor of $f=1.0$ is used. Note how the prepeak, although close to the correct position, does not appear to be fit so well as compared to Fig. 4.

In r space, the corresponding site-site radial distribution functions for these three case (Figs. 6 and 7) reveal some significant differences, both between themselves and with Fig. 3. In particular, it is clear that the data act as a major constraint on the extracted radial distribution functions. The

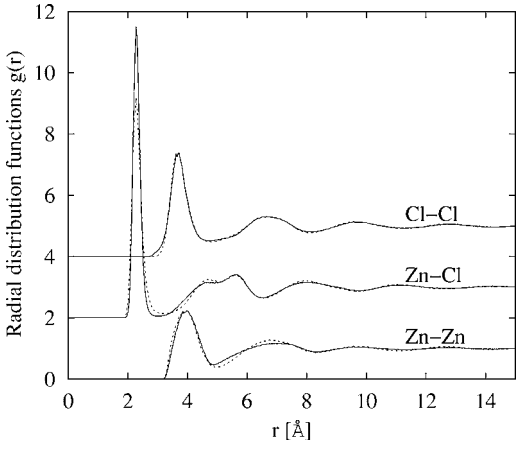

FIG. 6. Site-site radial distribution functions for molten $ZnCl_2$ as derived by EPSR using the case with feedback factor $f=0.4$ (solid line). The dashed line corresponds to the case with feedback factor $f=0.8$ as before. Note that the Zn-Zn peak is at slightly larger r values than the corresponding Cl-Cl peak, particularly for $f=0.4$. These radial distribution functions give the best fit to the supplied data according to Table IV, but there is clearly some uncertainty of the height of the main Zn-Cl peak, probably caused by the lack of diffraction data for $Q > \sim 10$ Å^{-1}.

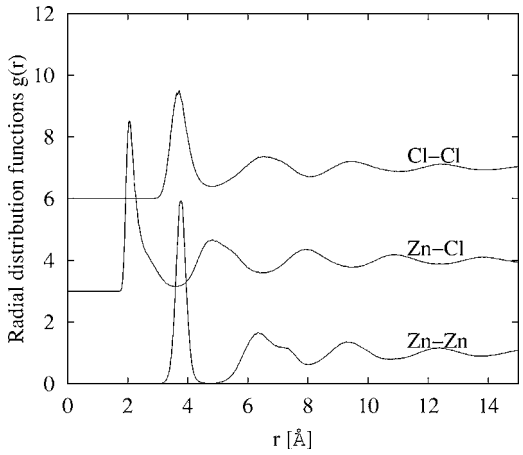

FIG. 7. Site-site radial distribution functions for molten $ZnCl_2$ as derived by EPSR using the case with 100% confidence in the data ($f=1.0$). Note that the position of Zn-Zn peak now occurs closer to the position of the corresponding Cl-Cl peak, and the subsequent minimum is also much more pronounced, compared to the fits with lower confidence. However, the fits to the diffraction data are far worse for this case (Fig. 5, Table IV) than when lower confidence is placed in the data (Fig. 4).

difference in quality of fit between $f=0.4$ and $f=0.8$ is only marginal according to Table IV and Fig. 4, yet small differences can be seen between the simulated distributions for these two cases (Fig. 6), particularly in the Zn-Cl and Zn-Zn distributions. In particular, the precise position of the first peak in the Zn-Zn distribution is quite sensitive to the quality of the fit. In neither of these fits, however, does it coincide in position with the first peak of the Cl-Cl distribution, as reported by Biggin and Enderby,[11] but is instead always at slightly larger r values. For $f=1.0$, on the other hand, where the fit to the diffraction data is markedly poorer, the Zn-Zn first peak is closer in position to the first peak of the Cl-Cl distribution, while the first peak in the Zn-Cl distribution develops a shoulder at high r and the second peak of this function in the distance range 4–6 Å does not have the double-hump appearance of the better fits at $f=0.4$ and $f=0.6$. Meanwhile, the Cl-Cl distribution for all the simulations looks rather similar. The $f=0.0$ simulation with full ionic charges has already captured the main features of this distribution. Changing from $f=0.4$ to $f=1.0$ does not appreciably alter the shape of the Cl-Cl RDF. Interestingly, a very recent high-precision study of $ZnCl_2$ glass using neutron diffraction[31] has produced radial distribution functions that are closely similar to those shown in Fig. 6. In particular, the Zn-Zn first peak is indeed found to be at slightly larger distances than the Cl-Cl first peak.

Obviously, one could go further and explore the ramifications of this study for the structure of molten zinc chloride and also compare the current outputs with earlier interpretations.[29,31–38] However, this is beyond the purpose of the present paper, which has to do with the way such data are analyzed; therefore, it is done separately.[39]

V. COMPARISON OF EPSR WITH REVERSE MONTE CARLO

Given that EPSR evolved from RMC it is useful to briefly compare the similarities and differences between the two approaches. The review by McGreevy[7] has covered many of the salient issues and these will not be repeated here. As McGreevy has discussed extensively,[7] EPSR, like RMC, is a tool for modeling the structure of a disordered material given a set of diffraction data. A few particular factors, however, need to be clarified.

It has sometimes been asserted that EPSR uses a purely pairwise additive interaction potential, and this therefore, limits its usefulness in systems where there are possibly covalent or other many-body forces. This statement is correct but needs to be qualified. For example, consider the case of rotation about a bond in a molecule. Such rotations will give rise to sharp peaks in the radial distribution function, even when the rotation is completely free. Clearly, pairwise forces would be not able to emulate that situation accurately, which requires definition of a torsion angle and involves at least four atoms. On the other hand, if there are such rotations present in particular molecules or if there are known many-body forces present, then these can be built into the reference potential in EPSR at the outset, if needed. The simulation can then be used to test the assumed form for the reference potential, so the structure refinement exercise can still lead to useful information. Alternatively, although it has been proven that for a pairwise additive system there is a unique relationship between the pair potential and the radial distribution function,[40] it appears that within the likely measuring and simulation uncertainties a range of pair potentials can, in fact, often be found that apparently give rise to the same structure.[27] Proving that an effective pair potential *cannot* be found for systems where covalent and many-body forces are present is extremely difficult and probably would have to be done on a case-by-case basis. Some tests indicate that under favorable conditions three-body correlations can be obtained accurately by EPSR,[27] and Howe and McGreevy came to a similar conclusion previously for RMC.[41] This point was made graphically recently[31] when the structure of two glasses, $ZnCl_2$ and $GeSe_2$, were shown to be closely similar, in spite of having quite different mechanisms for generating their respective interatomic forces, one partly ionic and partly covalent, the other primarily covalent. Experience with EPSR to date indicates that effective pairwise additive forces can be found in most cases of interest, and where this approximation breaks down there is always scope within the reference potential to include such extra nonpair terms as are needed.

At the same time it needs to be pointed out that RMC is strictly also only a pairwise additive method. In RMC, the quality of fit to the data is measured by $\chi^2=\Sigma_i\Sigma_Q([D_i(Q)-F_i(Q)]^2/\sigma_Q^2)$, where σ_Q is the statistical uncertainty on the data,[7] and $D_i(Q)$ are the data, and $F_i(Q)$ are the fits generated from the simulation box. The acceptance or rejection of an atom move is then based on

$$\Delta\chi^2 = \sum_i \sum_Q \frac{2[D_i(Q) - F_i(Q)]}{\sigma_Q^2} \Delta F_i(Q) + \sum_i \sum_Q \frac{\Delta F_i^2(Q)}{\sigma_Q^2}. \tag{17}$$

The second term in (17) is always positive for any atom move, but the first will be positive or negative, depending on whether the move makes χ^2 larger or smaller. Writing $\Delta F_i(Q) = 4\pi\rho \int_0^\infty r^2 \Sigma_j w_{ij} \Delta g_j(r) (\sin Qr/Qr) dr$, the first term in (17) can be rewritten

$$\Delta\chi^2 = 4\pi\rho \int_0^\infty r^2 \sum_i \left[\sum_j w_{ij} \Delta g_j(r) \right] c_i(r) + \sum_i \sum_Q \frac{\Delta F_i^2(Q)}{\sigma_Q^2}, \tag{18}$$

where $c_i(r) = \Sigma_Q (2[D_i(Q) - F_i(Q)]/\sigma_Q^2)(\sin Qr/Qr)$. Cast in this form, it becomes apparent that the change in χ^2 is driven by a Fourier transform of the differences between data and fits over the Q range of the data $c_i(r)$. This gives rise to two observations that often get overlooked. First the data are truncated in Q space and will likely contain statistical and systematic errors. These will, in turn, cause truncation and noise oscillations in $c_i(r)$, which then have the potential to bias the decision of whether to accept or reject the move. For example, a negative value of $\Delta\chi^2$ could be achieved when the oscillations in $\Sigma_j w_{ij} \Delta g_j(r)$ are in antiphase with the oscillations in $c_i(r)$. If $c_i(r)$ contains artifacts associated with truncation and noise, then it might well bias the choice of $\Delta g_j(r)$ to accept or reject, even though such artifacts have nothing to do with the structure of the material.

The effects of this on the outcome of a RMC simulation have never been rigorously explored, but the second point here is that since the change of χ^2 is driven by the functions $c_i(r)$ at each stage of the simulation, then the result is still determined only by pairwise additive interactions, since both the data and fit are purely pairwise additive functions of the atomic separations. As far as analyzing diffraction data is concerned, there is nothing intrinsic to RMC that says it will have any better chance of capturing many-body or covalent effects than any other simulation method with pairwise additive interactions.

In fact, the form (18) is closely analogous to the form used in EPSR (or any other Monte Carlo) simulation method. The differences are that in conventional Monte Carlo $\Delta\chi^2$ becomes a change in energy ΔU, $c_i(r)$ becomes the interaction potential $U^{(j)}(r)$ which then appears inside the sum over j, and of course there is no second term in the equation equivalent to (18). In EPSR the $U^{(j)}(r)$ is the sum of the reference potential and the empirical potential, but note that for the empirical potential the differences $D_i(Q) - F_i(Q)$ are accumulated over many iterations, via the fitting coefficients (15). In principle, the noise and truncation artifacts will be present in the empirical potential just as they are in RMC, but the Poisson functions used to generate the $U^{(j)}(r)$, as in Eq. (14), serve to minimize the extent to which such effects can be transferred. When a fit is achieved and the differences become small, the empirical potential retains the information on how the pair potential needs to be perturbed to get the fit. If the data were removed and the simulation left to run on its own, the empirical and reference potentials combined would hold the radial distribution functions and partial structure factors in the same forms they had when the data were present. In RMC when the differences become small, there is no record of what was needed to obtain the current atomic configuration, so that as soon as the data are removed, the configuration will rapidly collapse back into a random array of atoms.

Overall, therefore, although there are some technical differences, EPSR and RMC are actually closely analogous methods. The main differences are in the reference potential in EPSR, which serves to incorporate and test assumptions about how the atoms might be interacting, and in the empirical potential, which represents the perturbation to the reference potential needed to obtain a fit to the data. In RMC the reference potential is usually limited to a simple hard-core repulsive term to prevent atom overlap plus some coordination constraints if molecules or other known geometries are present. RMC, therefore, tries to minimize the amount of assumed knowledge at the outset.

VI. DISCUSSION

What is the "take-home" message from this study? Given the relatively good fit of the case where we set the feedback factor to zero, it would be rather easy to claim that the experiment has not told us much more than we could already glean from the simple ion model. Yet the parameters for the simple ion model, i.e., the reference potential, were themselves derived by referring to the diffraction data; thus, even at that level the experiment has had some impact. Obviously, by changing the parameters of the reference potential and other parameters in the simulation it might be possible to obtain still better fits to the data. However, this paper is primarily about the uniqueness of any inversion of isotope diffraction data, and, in place of a possibly endless search for the correct parameters for the reference potential, the empirical potential is used to guide the distribution of atoms as close as possible to that implied by the data. Using EPSR in the present case, several versions of the site-site RDFs have been generated from physical distributions of atoms that, to a greater or lesser extent, reproduce the experimental total differential cross-section data. Those that correspond to the best fits to the diffraction data show many features in common, whereas as the fit becomes worse, larger discrepancies show up between the extracted distributions. Assuming the data and their weighting factors are perfect, $f = 1.0$ does not necessarily lead to the best fit by the estimated RDFs. The Zn-Zn RDF seems particularly vulnerable to uncertainty, and this corresponds to its weak weighting in the total differential cross section (Table I). On the other hand, the Cl-Cl partial is strongly weighted in all the data sets, and thus, there is less variation in this function with different levels of fit.

Edwards and Enderby[10] refer to specific sum rules and limits that their solution to the inverse problem is forced to obey. In particular, there is the rule that $g(r) = 0$ near $r = 0$, and that the partial structure factors have to satisfy certain sum rule limits. The latter conditions are effectively the

statement that the density of points in reciprocal space cannot be less than zero. In EPSR, since the reference potential tends to $+\infty$ at low r; the condition on $g(r)$ is automatically satisfied. In addition, since all the calculated partial structure factors are derived from a three-dimensional array of atoms, the partial structure factors must, by definition, satisfy the condition on the density in reciprocal space. Hence, these sum rule conditions are satisfied in EPSR (as well as in RMC), automatically.

Obviously it would be possible to do further studies, for example, by choosing different feedback factors for different data sets or by choosing different reference potentials. However, the clear message delivered by this analysis is to be wary of any direct inversion of the data to give a set of partial structure factors, especially for weakly weighted contributions to the differential cross section. Without putting the data through a rigorous test, which involves ensuring that the reported site-site RDFs can be derived from a physical distribution of atoms or molecules, it is likely that important ambiguities in the experiment, which in the present case arise from the set of weight coefficients that appear in the formula for the total differential cross section, will be overlooked. The method described here has allowed the experimenter the opportunity to explore those ambiguities, and thus develop some confidence on what can and cannot be claimed in terms of the structure of the material in question.

VII. CONCLUSION

The notion of refining a three-dimensional model of a scattering system against a set of diffraction data is not new. It has been widely used for many decades by crystallographers and, more recently, RMC has been used to generate the structure of both disordered and crystalline materials.[8] Any crystallographer who attempted to publish a structure *without* reference to a physical model would not get very far. In the field of disordered materials, structure determination using three-dimensional atomistic modeling is increasingly being exploited as its power for identifying true and spurious structures becomes more widely understood.[7]

The present EPSR analysis of some old molten zinc chloride diffraction data has highlighted some of the uncertainties in structure reconstruction. By using different feedback factors, and by adopting different choices for the reference potential, one may generate a range of possible structures that are nonetheless quantitatively compatible with those data. The results could be a little unsettling because they may not agree with our prejudice. In particular, we may have to admit that some radial distribution functions cannot be reliably determined from the experiment, no matter how carefully we measure the data. The benefit of making this model is that it helps us to develop confidence in those results from the experiment that the data do support. At the same time it may help us to avoid making unsubstantiated statements about structures that are poorly determined or ambiguous.

ACKNOWLEDGMENT

I would like to thank numerous colleagues for a number of insightful comments on the contents of this paper.

[1] J. E. Enderby, D. North, and P. A. Egelstaff, Philos. Mag. **14**, 961 (1966).
[2] J.-P. Hansen and I. R. McDonald, *Theory of Simple Liquids*, 2nd ed. (Academic Press, New York, 1983).
[3] A. K. Soper, G. W. Neilson, J. E. Enderby, and R. A. Howe, J. Phys. C **10**, 1793 (1977).
[4] A. K. Soper and A. Luzar, J. Chem. Phys. **97**, 1320 (1992).
[5] D. L. Price and M.-L. Saboungi, in *Local Structure from Diffraction*, edited by S. J. L. Billinge and M. F. Thorpe (Plenum Press, New York, 1998), pp. 23–33.
[6] S. Ramos, A. C. Barnes, G. W. Neilson, D. Thiaudiere, and S. Lequien, J. Phys.: Condens. Matter **11**, A203 (2000).
[7] R. L. McGreevy, J. Phys.: Condens. Matter **13**, R877 (2001).
[8] D. A. Keen, L. Pusztai, and M. Dove, J. Phys.: Condens. Matter **17**, S1 (2005).
[9] A. K. Soper, Chem. Phys. **107**, 61 (1996).
[10] F. G. Edwards, J. E. Enderby, R. A. Howe, and D. I. Page, J. Phys. C **8**, 3483 (1975).
[11] S. Biggin and J. E. Enderby, J. Chem. Phys. **14**, 3129 (1981).
[12] M. P. Allen and D. J. Tildesley, *Computer Simulation of Liquids* (Oxford University Press, Oxford, 1987).
[13] D. Frenkel and B. Smit, *Understanding Molecular Simulation: From Algorithms to Applications* (Academic Press, New York, 1996).
[14] M. W. Johnson, P. Hutchinson, and N. H. March, Proc. R. Soc. London, Ser. A **282**, 283 (1964).
[15] L. E. Ballantine and J. C. Jones, Can. J. Phys. **51**, 1831 (1973).
[16] R. V. Gopola Rao and R. N. Joarder, Phys. Lett. **67A**, 71 (1978).
[17] W. Schommers, Phys. Rev. A **28**, 3599 (1983).
[18] D. Levesque, J. J. Weis, and L. Reatto, Phys. Rev. Lett. **54**, 451 (1985).
[19] L. Reatto, D. Levesque, and J. J. Weis, Phys. Rev. A **33**, 3451 (1986).
[20] G. Kahl and M. Kristufek, Phys. Rev. E **49**, R3568 (1994).
[21] A. P. Lyubartsev and A. Laaksonen, Comput. Phys. Commun. **121-122**, 57 (1999).
[22] J. Neuefeind, H. E. Fischer, and W. Schröer, J. Phys.: Condens. Matter **12**, 8765 (2000).
[23] R. L. McGreevy and L. Pusztai, Mol. Simul. **1**, 359 (1988).
[24] H. M. Rietveld, J. Appl. Crystallogr. **2**, 65 (1969).
[25] R. L. McGreevy and M. A. Howe, Phys. Chem. Liq. **24**, 1 (1991).
[26] M. A. Howe, R. L. McGreevy, L. Pusztai, and I. Borzsak I., Phys. Chem. Liq. **25**, 205 (1993).
[27] A. K. Soper, Mol. Phys. **99**, 1503 (2001).
[28] V. F. Sears, Neutron News **3**, 26 (1991).
[29] R. Triolo and A. H. Narten, J. Chem. Phys. **74**, 703 (1981).
[30] G. Hummer, D. M. Soumpasis, and M. Neumann, J. Phys.: Condens. Matter **6**, A141 (1994).
[31] P. S. Salmon, R. A. Martin, P. E. Mason, and G. J. Cuello, Nature

(London) **435**, 75 (2005).
[32] R. L. McGreevy and L. Pusztai, Proc. R. Soc. London, Ser. A **430**, 241 (1990).
[33] P. S. Salmon, Proc. R. Soc. London, Ser. A **437**, 591 (1992).
[34] M. Wilson and P. Madden, J. Phys.: Condens. Matter **5**, 6833 (1993).
[35] A. Bassen, A. Lemke, and H. Bertagnolli, Phys. Chem. Chem. Phys. **2**, 1445 (2000).
[36] J. Neuefeind, Phys. Chem. Chem. Phys. **3**, 3987 (2001).
[37] L. Pusztai and R. L. McGreevy, J. Phys.: Condens. Matter **13**, 7213 (2001).
[38] D. K. Belashchenko and O. I. Ostrovskii, Russ. J. Phys. Chem. **77**, 1111 (2003).
[39] A. K. Soper, Pramana, J. Phys. **63**, 41 (2004).
[40] R. L. Henderson, Phys. Lett. **49A**, 197 (1974); C. G. Gray and K. E. Gubbins, *Theory of Molecular Fluids. Volume I: Fundamentals* (Oxford University Press, London, 1984); R. Evans, Mol. Simul. **4**, 409 (1990).
[41] M. A. Howe and R. L. McGreevy, Phys. Chem. Liq. **24**, 1 (1991).